ORIGINAL PAPER

A comparative study of the chalcogen bond, halogen bond and hydrogen bond S⋯O/Cl/H formed between SHX and HOCl

Yi Fang · An Yong Li · Fei Yan Ma

Abstract Ab initio quantum chemistry methods were used to analyze the noncovalent interactions between HOCl and SHX (X = F, CN, NC, Cl, Br, NO$_2$, CCH, CH$_3$, H). Three energetic minimal configurations were characterized for each case, where the S center acts as a Lewis acid interacting with O to form a chalcogen bond, as well as a Lewis base interacting with Cl or H of HOCl to form halogen bond and hydrogen bond, respectively. An electronegative substituent such as F, CN, NC and NO$_2$ tends to form a stronger chalcogen bond, while an electropositive substituent such as CCH, CH$_3$ and H is inclined to form a more stable H-bonded complex. The chalcogen-bonded, halogen-bonded and H-bonded complexes are stabilized by charge transfers from Lp(O) to σ*(SX), from Lp(S) to σ*(ClO), and from Lp(S) to σ*(HO), respectively. As a result, the SHX unit becomes positively charged in halogen-bonded and hydrogen-bonded complexes but negatively charged in chalcogen-bonded complexes. Theory of atoms in molecules, natural bond orbital analysis, molecular electrostatic potential and localized molecular orbital energy decomposition analysis were applied to investigate these noncovalent bonds.

Y. Fang · A. Y. Li (✉) · F. Y. Ma
School of Chemistry and Chemical Engineering,
Southwest University, Tiansheng Road No.1, Beibei,
400715 Chongqing, People's Republic of China
e-mail: aylifnsy@swu.edu.cn

A. Y. Li
e-mail: ayli001@swu.edu.cn

Introduction

Noncovalent interactions play a significant role in super molecular chemistry, molecular biology, and materials science. The best known noncovalent interaction is the moderately directional hydrogen bond [1–5]. The dihydrogen bond is a special kind of hydrogen bond formed between a positively charged H-atom and another negatively charged H-atom [6]. Most noncovalent interactions may be classified as Lewis acid–Lewis base interactions [7] except for interactions such as those in methane dimers or between noble atoms. For a typical hydrogen bond, usually one positively charged H-atom is situated between two electronegative centers [8]. However, for a hydride bond, one negatively charged H-atom is situated between two electropositive centers [9]. So the hydride bond is also called an inverse hydrogen bond. From the paper by Grabowski [9], it has been accepted that the agostic bond is also a special kind of hydride bond. In summary, when a H-atom is connected with an electronegative center (O, N, S, etc.), it is positively charged and can act as a Lewis acid center; if the H-atom is bonded with an electropositive center (Na, Li, Mg, transition metals, etc.), it is negatively charged and so can be a Lewis base center.

In recent years, research into another noncovalent interaction—the halogen bond—has also expanded rapidly. Many studies have been performed on the C−X⋯Y halogen bond, where the C−X bond (X = Cl, Br, I) acts as the Lewis acid interacting with some electronegative center Y such as O or N atoms. A halogen atom covalently bonded with a carbon atom has a strong directional preference to interact with a Lewis base. This directional character of halogen bonds is often explained using the concept of anisotropic distribution of electron density around halogen nuclei [10]. The σ-hole concept was introduced and developed and can be applied to the halogen bond and other noncovalent interactions [11]. It is found that there is an area of positive electrostatic potential, called

the σ-hole, at the outmost region of electron density distribution of the halogen atom on the extension of the C−X bond [12, 13]. The σ-hole is formed due to electron deficience of a valence *p* orbital of the halogen atom in the C−X direction that participates in the σ(C−X) bond; it is surrounded by a region of negative electrostatic potential created by the other two lone *p* orbitals' electrons, as shown in Fig. 1. This determines the high directionality of halogen bonds because the linear geometry of the C−X⋯Y fragment provides maximal electrostatic attraction between the σ-hole and the Lewis base with negative electrostatic potential, and minimal repulsion between areas of negative electrostatic potential. It has been found that fluorine also has a σ-hole and so forms halogen bonds with Lewis bases when it is linked to a very electron-withdrawing group [14, 15] such as CN. Thus, all of the halogen atoms can act as both a Lewis acid and a Lewis base, and may participate in either a hydrogen bond or a halogen bond. This dual role is possessed not by hydrogen, which has only one shell, but by halogens with valence lone *p* orbitals. Some papers have compared the analogies and differences of hydrogen bonds and halogen bonds [16, 17]. The total energy of halogen bonding derived by Coulombic interaction also includes a significant contribution of polarization and dispersion interactions [18]. It should be noted that the presence of strong electron-withdrawing substituents results in an increase in the size of the σ-hole and binding energy [19]. This effect may be so significant that the surface of the whole halogen atom can become electropositive.

In addition to halogens F/Cl/Br/I, the two roles of Lewis acid and Lewis base may be possessed also by other atoms with a valence *p* orbital to form a polarized σ bond and valence lone orbitals such as N/P/As and O/S/Se of the main fifth and sixth groups. As they can covalently bond with electron-withdrawing atoms such as F, Cl, O and N, besides regions of negative electrostatic potential of lone *p* orbitals that can act as a Lewis base, these atoms also have a σ-hole of positive electrostatic potential as Lewis acids to form new kinds of noncovalent bonds—pnicogen bond and chalcogen bonds [20–28]—as shown in Fig. 1. The pnicogen bond has attracted great attention recently. These noncovalent interactions derived from Coulombic interactions between the σ-hole and negative sites are usually called σ-hole interactions.
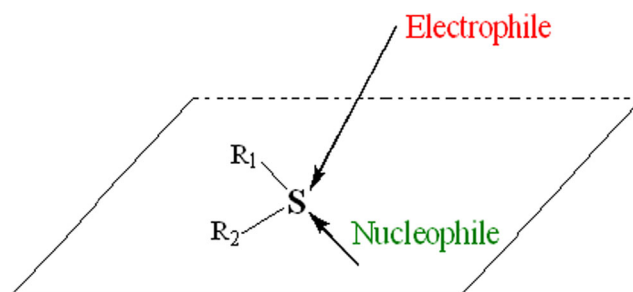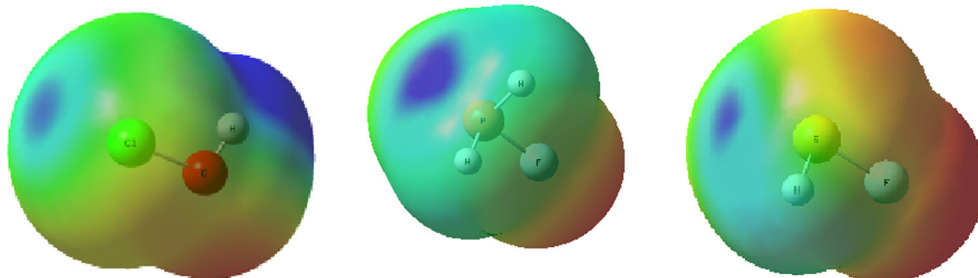

Scheme 1 Nucleophiles interact along the extension of covalent bonds R_1−S, while electrophiles interact above and below the molecular plane

Surveys of close contacts in divalent sulfide crystals revealed patterns analogous to those found for halides and phosphide. Nucleophiles interact along the extension of one of the covalent bonds R_1−S, but electrophiles interact above and below the molecular plane [29–31], as shown in Scheme 1. R_1 is an electronegative substituent while R_2 is an electropositive substituent. Because of the existence of the σ-hole and lone pair orbital, the sulfur atom of the molecule R_1R_2S may be involved in the formation of a chalcogen bond, a halogen bond, a pnicogen bond and a hydrogen bond. The chalcogen bond is formed by R_1−S acting as a Lewis acid interacting with an electronegative group, the other three bonds are formed by the lone pairs of S acting as Lewis bases interacting with the σ-hole of F/Cl/Br/I−C, P−X and H−X, where X is an electronegative group. The literature describing these kinds of bonds is abundant, and some recent papers have compared these types of noncovalent interactions. However, could substituent effects be used to preferentially select the type of bond formed?

To answer this question, we have investigated a series of complexes involving molecules HXS and HOCl, with substituent X = F, NC, Cl, Br, NO_2, CN, CCH, CH_3, and H. Because both SHX and HOCl have σ-holes and lone pairs, in principle three types of bonds, S⋯O chalcogen bond, S⋯H hydrogen bond, S⋯Cl halogen bond, could be formed, as shown in Scheme 2. This paper reports a theoretical study on the chalcogen bond, halogen bond, and hydrogen bond in the HOCl:SHX system, and on substituent effects on the S⋯O, S⋯Cl and S⋯H noncovalent bonds. We present the structures, binding energies, bonding properties, and vibrational frequencies

Fig. 1 Molecular electrostatic potentials (MEPs) of the free monomers HOCl, FH_2P and SHF on an isosurface (0.0004 e a.u.$^{-3}$) of electron density. The range of electrostatic potential is from −0.02 a.u. (*red*) to +0.06 a.u. (*blue*)

Scheme 2 The three types of bond formed in the HOCl:SHX system

Chalcogen bond   **Halogen bond**   **Hydrogen bond**
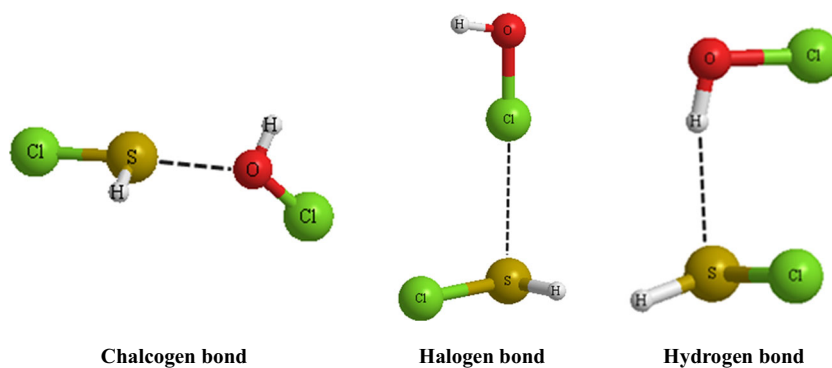
of these complexes. The concepts of rehybridization and hyperconjugation [32, 33], and intra- and inter-hyperconjugations [34] have been well applied to interpret red-shifted and blue-shifted hydrogen bonds, and have also been shown to be applicable to halogen bonds. Here, we investigated whether these theories are suitable for chalcogen bonds. We hope this study may inspire experimental scientists to affirm the existence of these complexes in the future.

Computational methods

All quantum chemistry calculations were performed using the Gaussian09 program [35]. The structures were first optimized at the MP2 level with the aug-cc- pVDZ basis set and then frequency calculations were performed to confirm the geometries obtained corresponding to true minima. The equilibrium geometry was further refined using MP2/aug-cc-pVTZ. A single-point energy was computed using the MP4(SDQ)/aug-cc-pVTZ//MP2/aug-cc-pVTZ method. The basis set superposition error (BSSE) in the energies of the complexes was eliminated by the standard counterpoise (CP) correction method of Boys and Bernardi [36].

Electron densities of the monomers and complexes were analyzed using the theory of atoms in molecules (AIM) [37–40] and employing the AIMAll program [41]. The natural bond orbital (NBO) method [42] was used to obtain atomic charges and to analyze the stabilizing charge transfer

interactions in these binary complexes. The NBO-5 program [43] was used for NBO calculations.

The localized molecular orbital energy decomposition analysis (LMOEDA) at the MP2/aug-cc-PVTZ level was used to partition the interacting energy E_{int} into various terms [44], including electrostatic interaction energy E_{es}, exchange energy E_{ex}, repulsion energy E_{rep}, polarization energy E_{pol} and dispersion energy E_{disp}, thus $E_{int} = E_{es} + E_{ex} + E_{rep} + E_{pol} + E_{disp}$. These calculations were performed using GAMESS program (version-2013 R1) [45].

Results and discussion

Structures and bonding

The minimum-energy configurations of the complexes SHX:HOCl with S···O, S···Cl, S···H interactions optimized by use of MP2/aug-cc-PVDZ and MP2/aug-cc- pVTZ methods have similar geometries, the detailed structural parameters are listed in Tables 1, 2 and 3. Although there are many minima on the SHX:HOCl potential energy surfaces, we restricted our searches to those regions at which a S···O chalcogen-bond, S···Cl halogen-bond or S···H hydrogen-bond is formed, S acts as the Lewis acid center in the chalcogen-bond but as the Lewis base in the other two cases.

The chalcogen-bonded, halogen-bonded and hydrogen-bonded complexes can be structurally distinguished from each

Table 1 Geometrical parameters of chalcogen bond structures (length in Å; angles in °)

HSX:HOC	mp2/aug-cc-pVDZ								mp2/aug-cc-pVTZ							
	SX	SH	OH	OCl	S···O	XSO	HSO	XSOH	SX	SH	OH	OCl	S···O	XSO	HSO	XSOH
F	1.687	1.350	0.976	1.735	2.651	166.8	72.5	117.3	1.643	1.336	0.970	1.699	2.639	166.6	71.6	−131.5
CN	1.718	1.351	0.975	1.734	2.973	158.4	63.6	−133.3	1.699	1.338	0.969	1.699	2.973	155.6	60.9	−137.3
NC	1.701	1.350	0.975	1.735	2.786	163.7	69.1	−137.3	1.673	1.337	0.970	1.699	2.781	163.2	68.2	−130.2
Cl	2.086	1.350	0.975	1.735	2.796	164.6	70.3	−117.4	2.047	1.337	0.970	1.699	2.801	164.7	69.5	−133.0
Br	2.235	1.350	0.975	1.735	2.836	163.7	69.8	−137.3	2.194	1.337	0.970	1.699	2.839	163.9	69.1	−132.4
NO₂	1.808	1.350	0.975	1.735	2.837	162.8	70.0	−143.8	1.779	1.337	0.970	1.699	2.828	161.3	68.3	−140.1

Table 2 Geometrical parameters of halogen bond structures (length in Å; angles in °)

HSX:HOCl	mp2/aug-cc-pVDZ								mp2/aug-cc-pVTZ							
	SX	SH	OH	OCl	S···Cl	XSCl	OClS	HSXCl	SX	SH	OH	OCl	S···Cl	XSCl	OClS	HSXCl
F	1.676	1.354	0.974	1.741	3.202	98.9	177.2	−91.8	1.631	1.340	0.969	1.707	3.122	96.1	176.8	−89.5
CN	1.716	1.354	0.975	1.736	3.259	83.2	173.4	−88.8	1.697	1.341	0.969	1.701	3.237	82.3	172.1	−83.5
NC	1.693	1.353	0.975	1.738	3.220	86.3	173.7	−86.3	1.664	1.340	0.969	1.702	3.183	83.0	170.4	−87.8
Cl	2.074	1.353	0.974	1.742	3.149	93.5	177.8	−93.6	2.036	1.340	0.969	1.707	3.098	92.3	176.8	−92.2
Br	2.225	1.354	0.974	1.743	3.127	92.8	177.8	−92.8	2.185	1.340	0.969	1.708	3.089	91.7	176.9	−91.6
NO$_2$	1.817	1.353	0.974	1.735	3.268	75.7	168.5	−91.1	1.786	1.340	0.969	1.700	3.242	74.9	166.6	−89.6
CCH	1.715	1.354	0.974	1.743	3.153	92.1	177.9	−91.4	1.694	1.340	0.969	1.707	3.116	90.5	177.1	−89.3
CH$_3$	1.833	1.350	0.974	1.753	3.018	86.4	171.9	−96.0	1.815	1.337	0.968	1.718	2.97	87.0	171.7	−93.4
H	1.350	1.350	0.974	1.744	3.177	91.8	177.1	−91.9	1.337	1.337	0.968	1.709	3.136	90.0	176.5	−90.0

other by the values of the bonding angles X−S···O, X−S···Cl and X−S···H. For the chalcogen bond, the angle X−S···O is close to 180°, but for the halogen and hydrogen bonds, the X−S···Cl/H angles are close to 90° (see Scheme 2 and Tables 1–3). This confirms that S plays different roles in the chalcogen bond and the halogen/hydrogen bonds; in the former, S uses its σ-hole as a Lewis acid but in the latter it uses its lone pair as a Lewis base. The interaction distance S···H (2.23–2.48 Å) of the H-bond is the shortest among the three kinds of bonds, followed by the chalcogen bond S···O (2.78–2.97 Å) and the

Table 3 Geometrical parameters of hydrogen bond structures (length in Å; angles in °)

HSX:HOCl	mp2/aug-cc-pVDZ								mp2/aug-cc-pVTZ							
	SX	SH	OH	OCl	S···H	XSH	OHS	HSXH	SX	SH	OH	OCl	S···H	XSH	OHS	HSXH
CN	1.718	1.354	0.978	1.732	2.508	93.0	153.5	−106.0	1.819	1.342	0.973	1.696	2.498	89.3	149.1	−110.1
NC	1.692	1.354	0.978	1.731	2.487	93.5	155.6	−104.6	1.664	1.341	0.974	1.695	2.461	93.8	152.1	−107.1
Cl	2.073	1.354	0.982	1.730	2.356	88.6	169.5	−97.9	2.035	1.341	0.977	1.694	2.341	90.8	162.6	−100.5
Br	2.225	1.354	0.982	1.730	2.335	87.5	170.4	−96.9	2.185	1.340	0.978	1.694	2.325	88.7	163.2	−99.4
NO$_2$	1.831	1.354	0.979	1.732	2.494	91.3	159.7	−98.3	1.799	1.340	0.973	1.697	2.479	92.1	157	−98.7
CCH	1.716	1.354	0.981	1.730	2.377	89.1	166.3	−99.5	1.696	1.341	0.976	1.694	2.363	88.8	162.6	−100.6
CH$_3$	1.836	1.351	0.988	1.729	2.250	87.8	163.6	−95.5	1.819	1.338	0.984	1.693	2.232	89.3	163.2	−95.3
H	1.351	1.351	0.984	1.729	2.334	91.2	171.2	−91.2	1.338	1.338	0.980	1.693	2.309	89.5	168.3	−89.5

Table 4 Interaction energies (kJ mol^{-1}) with basis set superposition error (BSSE) correction. pvdz: mp2/aug-cc-pVDZ, pvtz: mp2/aug-cc-pVTZ, MP4: MP4(SDQ)/AUG-CC-pVTZ// mp2/aug-cc-pVTZ

X	Chalcogen bond			Halogen bond			Hydrogen bond		
	pvdz	pvtz	MP4	pvdz	pvtz	MP4	pvdz	pvtz	MP4
F	−16.39	−17.31	−17.65	−7.46	−9.29	−9.42	–	–	–
CN	−11.81	−12.82	−15.47	−7.43	−9.03	−9.32	−7.45	−9.86	−10.19
NC	−15.19	−16.05	−17.2	−7.92	−9.72	−9.44	−7.73	−10.46	−11.41
NO$_2$	−12.77	−14.22	−15.86	−7.7	−9.63	−8.54	−10.07	−12.5	−11.02
Cl	−12.66	−13.19	−11.92	−8.87	−10.82	−7.29	−13.11	−10.82	−13.99
Br	−11.62	−12.09	−7.94	−9.39	−11.33	−6.67	−14.04	−17.58	−13.70
CCH	–	–	–	−9.22	−10.81	−10.07	−14.19	−17.05	−17.21
H	–	–	–	−9.42	−10.68	−7.73	−18.68	−21.44	−18.98
CH$_3$	–	–	–	−14.49	−16.74	−11.19	−25.05	−28.63	−25.17

Table 5 Electrostatic (E^{ele}), exchange (E^{ex}), repulsion (E^{rep}), polarization (E^{pol}), and dispersion (E^{disp}) terms as well as the total interaction energy (E^{int}) calculated using the MP2/aug-cc-pVTZ method. All energies are in units of kcal mol^{-1}

X	Chalcogen bond						Halogen bond						Hydrogen bond					
	E^{ele}	E^{ex}	E^{rep}	E^{pol}	E^{disp}	E^{int}	E^{ele}	E^{ex}	E^{rep}	E^{pol}	E^{disp}	E^{int}	E^{ele}	E^{ex}	E^{rep}	E^{pol}	E^{disp}	E^{int}
F	−7.64	−12.23	21.87	−2.98	−3.96	−4.94	−5.45	−11.84	20.96	−2.51	−3.93	−2.78	–	–	–	–	–	–
CN	−3.8	−5.13	8.86	−0.98	−2.54	−3.6	−3.2	−8.28	14.25	−1.42	−4.02	−2.68	−2.8	−9.09	15.79	−2.32	−4.74	−3.16
NC	−5.39	−8.13	14.28	−1.75	−3.55	−4.53	−3.83	−9.46	16.37	−1.72	−4.21	−2.87	−3.82	−9.31	16.26	−2.57	−3.88	−3.32
Cl	−5.14	−8.69	15.18	−1.68	−3.48	−3.82	−5.45	−12.58	22.12	−2.55	−4.76	−3.21	−5.15	−10.97	19.44	−3.52	−4.78	−4.98
Br	−4.7	−8.33	14.47	−1.48	−3.46	−3.5	−5.63	−13.28	23.29	−2.64	−5.11	−3.36	−5.33	−11.89	20.99	−3.73	−5.33	−5.29
NO$_2$	−5.37	−7.33	12.86	−1.83	−2.39	−4.06	−3.19	−8.66	15.02	−1.43	−4.71	−2.98	−3.02	−9.78	17.15	−2.47	−5.97	−4.09
CCH	–	–	–	–	–	–	−4.75	−11.8	20.3	−2.5	−4.38	−3.14	−4.78	−10.44	18.39	−3.36	−4.81	−4.99
CH$_3$	–	–	–	–	–	–	−10.08	−20.9	37.46	−4.9	−6.49	−4.91	−10.14	−16.69	29.89	−5.54	−5.55	−8.03
H	–	–	–	–	–	–	−5.89	−12.37	21.73	−2.57	−3.96	−3.06	−7.8	−12.76	22.81	−4.18	−4.03	−5.96

halogen bond S···Cl (3.12–3.24 Å). The halogen bond O−Cl···S is almost linear, and the hydrogen bond O−H···S has a 10–30° deviation from linearity.

It has been proposed [27, 28] that R−H···Y hydrogen bonding should be classed as one kind of σ-hole noncovalent interaction, since the covalently bonded hydrogen also has a σ-hole on the extension of the R−H bond. A difference between the σ-hole of hydrogen and those of Group V–VII atoms is that the former is more hemispherical while the latter are more narrowly focused. Thus, the hydrogen bonding tends to be less directional overall than other σ-hole interactions such as halogen, pnicogen and chalcogen bonds.

The preferred type of intermolecular bonds can be selected by changing the substituent. For a very electronegative and strongly electron-withdrawing substituent such as X = F, only chalcogen-bonded and halogen-bonded complexes are formed, because the σ-hole at S is enhanced but the nucleophilicity above and below the molecular plane is decreased so that it becomes a good electron acceptor for the formation of the chalcogen bond S···O but a poor electron donor for the halogen bond S···Cl and especially the hydrogen bond S···H. For a very electropositive group such as X = CCH, H and CH$_3$, only halogen-bonded and hydrogen-bonded structures are formed, because these electropositive substituents essentially destroy the σ-hole by increasing the electron density and nucleophilicity above and below the molecular plane such that the S atom becomes a stronger electron donor for the halogen/hydrogen bond but cannot act as an electron acceptor for a chalcogen bond.

Interaction energies

Table 4 lists the BSSE-corrected interaction energies calculated using the MP2 and MP4(SDQ) methods with the correlation consistent basis sets. From the data in this table, it is possible to answer the question in the Introduction. For the more electron-withdrawing substituents X = F/NC/NO$_2$/CN, the chalcogen bond is the strongest of the three noncovalent bonds, but for the more electropositive substituents X = CCH/H/CH$_3$ and Br, the hydrogen bond is strongest. For X = Cl, the chalcogen and hydrogen bonds can be equally strong. In all three systems, the halogen bond is the weakest bond. Thus, electronegativity and the electron-withdrawing ability of the substituent bonded to sulfur determine the binding energies of the resulting complexes and the type of the formed noncovalent bond. In other words, an electronegative substituent X prefers a chalcogen bond but an electropositive substituent prefers a hydrogen bond. The bonding energy of the chalcogen bond decreases but the energies of the halogen and hydrogen bonds increase in decreasing order of the electronegativity and electron-withdrawing ability of the substituent X. This law is particularly obvious for the simple substituents F/Cl/Br/H/CH$_3$, and can be

Table 6 The maximal value ($V_{S,max}$, kcal mol^{-1}) of positive electrostatic potentials and the minimal value ($V_{S,min}$, kcal mol^{-1}) of negative electrostatic potentials on the van der Waals isosurface of the S atom in SHX calculated at the mp2/aug-cc-pVDZ level

Monomer	SHF	SHCl	SHBr	SH$_2$	SHCH$_3$	SHNO$_2$	SHCN	SHNC	SHCCH
$V_{S,max}$ S σ hole	42.0	36.3	32.5	–	–	52.5	43.5	21.2	27.1
$V_{S,min}$ S lone pair	−10.4	−11.7	−12.5	−18.9	−22.8	−18.7	−0.5	−5.4	−13.3

interpreted easily by considering the effects of the substituent on the σ-hole and lone pairs of S.

To gain a deeper understanding of the nature of the interactions in these complexes, a localized molecular orbital energy decomposition analysis (EDA) was performed using the MP2/aug-cc-pVTZ method; the various terms of the interaction energy have been gathered in Table 5. The results for three kinds of noncovalent interactions have some similarity. The term with the largest magnitude is always the repulsion term. The exchange term is the largest among the four attractive terms (electrostatic, exchange, polarization and dispersion) and accounts for 40–50 % of the total attractive energy, the electrostatic and dispersion energies are also important and contribute 40–50 % of the attractive energy, the polarization term is the smallest and accounts only for 8–15 % of the attractive energy. The nonignorable polarization energy indicates that there is a remarkable induced dipole interaction between monomers, which is consistent with the obvious charge transfer from the Lewis base to the Lewis acid in these complexes (see Table 7 below).

Electrostatic potentials

It has been shown [27, 28] that the σ-hole noncovalent interactions of Group IV–VII atoms such as halogen, chalcogen and pnicogen bonds and also the hydrogen bond can be explained in terms of Coulombic interactions between positive σ-holes on the atom covalently bonded to an electronegative

group and negative sites. The electrostatic potential is a crucial property in explaining and predicting these noncovalent interactions. The molecular electrostatic potential (MEP) is a physical observable and can be measured experimentally or calculated theoretically using the following formula.

$$V(\mathbf{r}) = \sum_A \frac{Z_A}{|\mathbf{R}_A - \mathbf{r}|} - \int \frac{\rho(\mathbf{r}')}{|\mathbf{r} - \mathbf{r}'|} d^3\mathbf{r}' \qquad (1)$$

$V(\mathbf{r})$ is the potential created at any point $\mathbf{r}$ by the nuclei and electrons of the molecule; Z_A is the charge on nucleus A, located at $\mathbf{R}_A$, and $\rho(\mathbf{r})$ is the molecule's electronic density. A free, ground-state atom has a spherically symmetrical electronic charge distribution and its electrostatic potential is positive everywhere. But the atom involved in a covalent bond has an anisotropic electron density distribution; due to the electron charge polarized toward the bond region, the outer portion on the extension of the covalent bond has a more positive electrostatic potential, called the σ-hole.

The σ-hole interactions are determined by, and correlate strongly with, the strengths of the σ-hole (the Lewis acid) and the negative site (the Lewis base), which are represented by the local most positive electrostatic potential $V_{S,max}$ of the σ-hole and the local most negative potential $V_{S,min}$ of the negative site, respectively [27, 28], on a molecular isodensity surface [usually the van der Waals isosurface (0.001 a.u.)]. Large $V_{S,max}$ and $|V_{S,min}|$ values produce large interaction energies.

Table 7 Charge transfer (CT, e), second-order perturbation energy ($E^{(2)}$ kcal mol^{-1}) corresponding to the orbital interactions Lp(O)→σ*(SX), Lp(S)→σ*(ClO) and Lp(S)→σ*(OH), respectively, for the chalcogen, halogen and hydrogen bonds, calculated using the mp2/aug-cc -pVTZ method; the selected vibration frequencies shifts ($\Delta\nu$, cm^{-1}) by MP2/aug-cc-pVDZ and the corresponding bond changes (Δr, Å) obtained by MP2/aug-cc-pVTZ upon complexation

X	Chalcogen bond				Halogen bond				Hydrogen bond			
	CT	$E^{(2)}$	$\Delta\nu$(SX)	Δr(SX)	CT	$E^{(2)}$	$\Delta\nu$(OCl)	Δr(OCl)	CT	$E^{(2)}$	$\Delta\nu$(OH)	Δr(OH)
F	0.013	6.70	−22.5	0.009	−0.023	6.65	−23.5	0.010	–	–	–	–
CN	0.005	1.51	−4.3	0.002	−0.007	2.75	−15.7	0.004	−0.004	4.02	−82.8	0.005
NC	0.010	4.38	−14.7	0.007	−0.012	3.90	−17.2	0.005	−0.011	6.10	−90.2	0.005
Cl	0.009	4.29	−12.4	0.008	−0.007	2.75	−27.4	0.010	−0.004	11.45	−156.1	0.009
Br	0.008	3.88	−10.0	0.007	−0.019	5.99	−29.5	0.011	−0.023	11.78	−169.0	0.009
NO$_2$	0.010	3.79	6.5	−0.005	−0.007	2.70	−10.5	0.003	−0.010	5.28	−93.7	0.005
CCH	–	–	–	–	−0.017	4.92	−28.6	0.010	−0.019	8.68	−149.1	0.008
CH$_3$	–	–	–	–	−0.036	10.16	−55.7	0.021	−0.041	19.85	−295.8	0.016
H	–	–	–	–	−0.021	6.05	−31.2	0.012	−0.029	14.65	−206.5	0.011

Table 8 Changes in natural atomic charges, occupancy on σ*(SX), polarization percentages and the *s* characters involved in the σ(SX) bond of S and X for the chalcogen bond, calculated using the MP2/aug-cc-pVTZ method

X	$\delta q(S)$	$\delta q(X)$	$\delta pol(X)$	$\delta pol(S)$	$\delta s(X)$	$\delta s(S)$	$\delta\sigma^*(X\text{-}S)/me$
F	−0.0062	−0.0181	0.70 %	−0.77 %	0.91 %	−0.77 %	15.03
CN	−0.0002	0.0025	0.43 %	−0.43 %	0.28 %	−0.49 %	3.33
NC	−0.0026	0.0027	0.57 %	−0.57 %	0.45 %	−0.82 %	7.93
Cl	0.0052	−0.0222	0.95 %	−0.95 %	0.46 %	−0.61 %	9.93
Br	0.0085	−0.024	1.04 %	−1.04 %	0.39 %	−0.54 %	9.17
NO$_2$	0.0131	−0.0092	0.93 %	−0.93 %	0.83 %	−0.42 %	−1.51

In our systems XHS:HOCl, the sulfur has both a σ-hole and two lone pairs, thus a local maximum $V_{S,max}$ on the extension of the XS bond and two identical local minima $V_{S,min}$ above and below the XHS molecular plane, which are listed in Table 6 for a series of substituents X. The substituent X strongly influences the σ-hole and the lone pairs. Since σ-holes are due to polarization of an atom's electronic charge toward the covalent bonds that it forms, any factor that enhances this polarization will strengthen the σ-hole. We see that the σ-hole becomes weaker and the lone pair stronger in the order of the simple substituents X = F, Cl, Br, H and CH$_3$. In the chalcogen bonding complexes, the Lewis base does not vary, it is always the oxygen of HOCl, but the σ-hole on S of the HXS changes with the substituent X. There is an overall trend that a more electronegative and electron-withdrawing substituent produces a more positive σ-hole and leads to a larger interaction energy, and vice versa. In the halogen/hydrogen bonding complexes, the chlorine/hydrogen σ-hole of HOCl is the same in each complex, but what varies is the strength of the negative region associated with the sulfur (its $V_{S,min}$). In these complexes, a more electron-withdrawing substituent X in HSX will diminish $|V_{S,min}|$ of the negative site of the sulfur in HSX, and overall produces smaller interaction energies of the halogen and hydrogen bonds. These laws are obvious for the simple substituents X = F, Cl, Br, H and CH$_3$. For X = H and CH$_3$ there is no σ-hole and so no chalcogen bond; for X = F there are the weakest lone pairs such that the hydrogen bond cannot be formed; for the other substituents X = −NO$_2$, −NC, −CN and −CCH, the effect of their π bonds on the σ-hole and lone pairs is complex and has no obvious law, which should be studied in detail separately.

Charger transfer, electron density and frequency shifts

The σ-hole interactions were considered as electrostatically driven and can be interpreted by electrostatics, polarization and dispersion [27, 28]. The polarization and dispersion are seen as intrinsic components of the Coulombic interaction. Polarization is simply the shifting of electron density from the Lewis base to the Lewis acid—the σ-hole—thus stabilizing the complex. Taking another viewpoint, i.e., that of a mathematical model, the polarization and charger transfer can be interpreted using the concept of orbital interactions and hyperconjugations. NBO analysis is a standard tool for doing this. Tables 7 and 8 list the results of NBO and AIM analyses performed at the MP2/Aug-cc-pVTZ level.

In the chalcogen-bonded complexes there is an obvious charge transfer (CT) from the Lewis base HOCl to the Lewis acid HXS, but in the halogen-bonding and H-bonding structures, there are larger charge transfers in the opposite direction from the Lewis base HXS to the Lewis acid HOCl. These charge transfers are caused by the significant intermolecular orbital hyperconjugation interactions Lp(O) → σ*(SX) for the chalcogen bond, Lp(S) → σ*(ClO) for the halogen bond, and Lp(S) → σ*(OH) for the hydrogen bond. Large CT corresponds to large second-order perturbation energy $E^{(2)}$ of the hyperconjugation. These charge transfers can interpret the bond elongation and frequency red shift of the bonds SX, OCl and OH in the Lewis acids, respectively, for the chalcogen, halogen and hydrogen bonds. An exception is that, in the chalcogen-bonding complex with X = NO$_2$, the N−S bond contracts and its frequency blue shifts. This phenomenon should be interpreted separately. The frequency red shifts of

Fig. 2 **a** Intramolecular hyperconjugations n(O)s→σ*(SN) in HSNO$_2$. **b** Coupling of intramolecular and intermolecular hyperconjugations in the chalcogen complex NO$_2$HS⋯OHCl

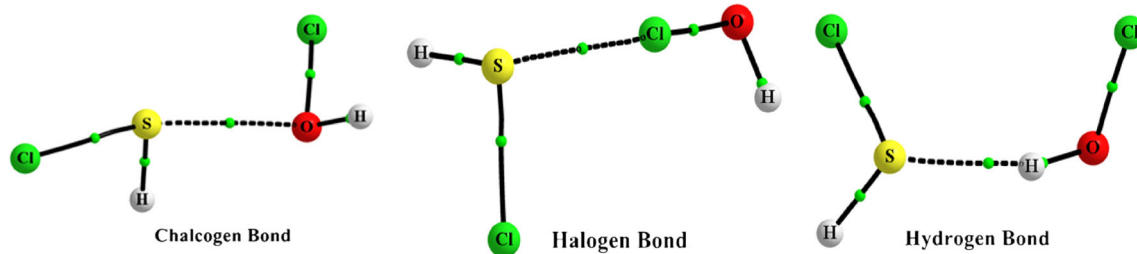(a)   (b)
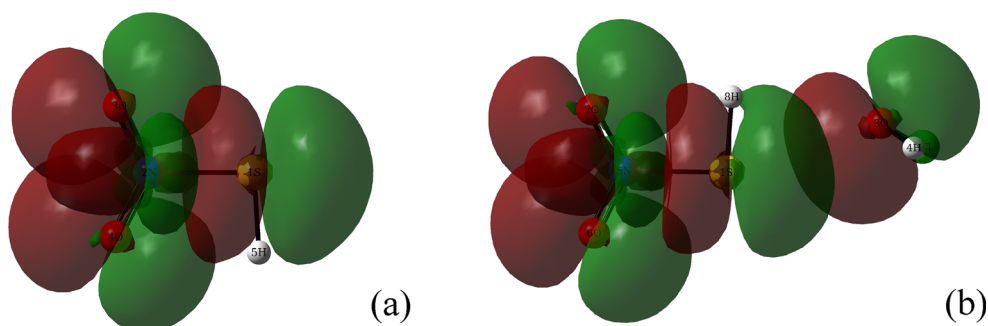
Fig. 3 Molecular graphs of the three SHCl···HOCl complexes at the MP2/aug-cc-pVDZ level. *Small green balls* Bond critical points (BCPs)

the OH bond in the H-bonding complexes are the largest among the three kinds of complexes, corresponding to the largest binding energies.

The theory of repolarization and rehybridization and hyperconjugation proposed by Weinhold and Alabugin [32] has been used to interpret the red and blue shift character of H-bonds. Recently, it was shown that this theory is also valid for halogen bonds [46]. Here, we test this theory for the chalcogen bond. The NBO data show that formation of the chalcogen bond also results in repolarization of the X–S bond, similar to repolarization of the X–H bond in a H-bond, the X atom becomes more electronegative and the S atom more electropositive in the complexes than in the monomer, see Table 8. For the NBO bonding orbital $\sigma(X–S) = c_1 h(X) + c_2 h(S)$, the probability $|c_1|^2$ [polarization percentage pol(X)] of electrons in $\sigma(X–S)$ appearing in the hybrid $h(X)$ increases but the probability $|c_2|^2$ [polarization percentage pol(S)] appearing in the hybrid $h(S)$ decreases in complexes compared with the monomer HXS. According to Bent's rule [47], repolarization leads to rehybridization of the X and S hybrids, thus the *s*-orbital percentage of the hybrid $h(X)$ increases but that of $h(S)$ decreases in the complexes compared with the monomer. So, the repolarization and rehybridization of the X–S bond in the chalcogen

bonding are completely similar to those of the X–H bond in the H-bond, and the C–Cl/Br/I bond in the halogen bond. Hyperconjugation causes XS/OCl/OH bond elongation and frequency red shift but rehybridization leads to bond contraction and frequency blue shift. Competition between these two effects determines the ultimate result. Thus perhaps we could say that, for the chalcogen-bonded complex with X = NO$_2$, rehybridization is predominant such that the NS bond contracts and its frequency blue shifts. For the other complexes the converse is the case.

In practical applications, it is difficult to determine which of rehybridization and hyperconjugation is predominant. In most cases, such as in the systems examined here, the theory of inter- and intra-molecular hyperconjugations [34] is more suitable for interpreting the frequency shifts. In the chalcogen bonded systems with X = F, Cl, Br, CN and NC, the only important factor is the intermolecular hyperconjugation n(O) → σ*(SX), which increases occupancy on σ*(S-X), as shown in Table 8, and so results in the elongation and frequency red shift of the SX bond. However, for the chalcogen bonding complex with X = NO$_2$, the case is very different. In the monomer HSNO$_2$, one lone pair orbital of each O atom on NO$_2$ has a large overlap with σ*(SN) of SHNO$_2$, so there are two strong intramolecular

Fig. 4 Relationship between the inter-fragment distance (Å) and electron densities (a.u.) at inter-BCPs for S···O/Cl/H interactions
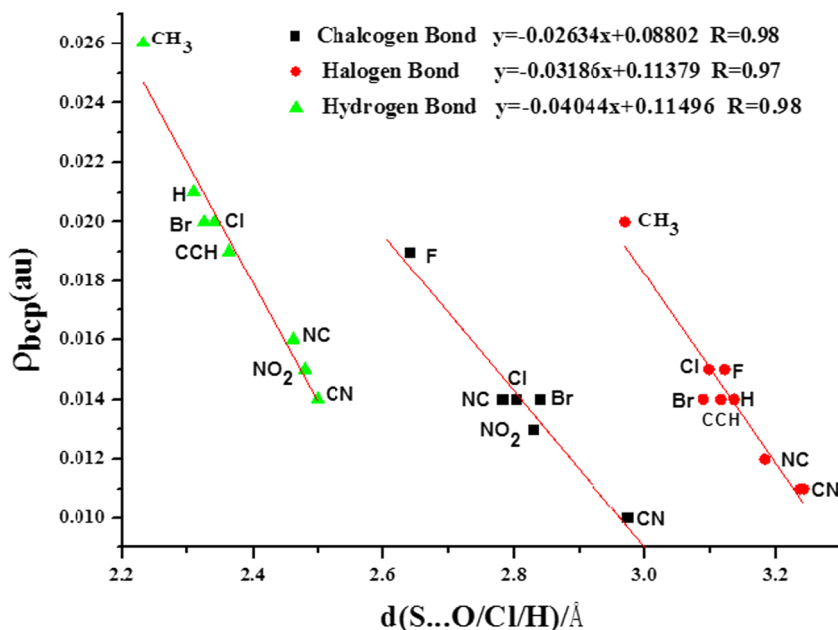
hyperconjugations n(O) → σ*(SN) with second-order perturbation energies of 22.9 and 27.1 kcal mol^{-1}, which transfers electron density from the lone pairs n(O) of NO_2 to σ*(SN) such that the occupancy on σ*(SN) is up to 0.1125e, as shown in Fig. 2a. Upon formation of the X−S⋯O chalcogen bond, the intermolecular hyperconjugation n(O) → σ*(SN) requires some overlap between n(O) of HOCl and σ*(SN). As a result, the overlap between σ*(SN) and the lone pairs of NO_2 decreases such that the intramolecular hyperconjugations decrease, and the second-order perturbation energies $E^{(2)}$ drop to 20.5 and 24.6 kcal mol^{-1}. Some electron density on σ*(SN), originally coming from n(O) of NO_2, now flows back to n(O) of NO_2, as shown in Fig. 2b. The final net result is that the occupancy on σ*(SN) decreases by 1.51me, which leads to shortening and the frequency blue shift of the S−N bond.

The AIM analysis showed that the intermolecular bond critical points (inter-BCP) are situated between S⋯O, Cl⋯S and H⋯S, respectively, for the chalcogen, halogen and hydrogen bonds, as plotted in Fig. 3. The electron density ρ at the inter-BCPs is 0.01–0.026 a.u., the Laplacian $\nabla^2\rho$ is 0.04–0.08 a.u., and the electron energy density, H, is a positive value less than 0.1 a.u. Thus these noncovalent bonds are weak closed-shell interactions and have no covalent character. The electron densities at the inter-BCPs have good linear correlation with the inter-fragment distance d(S⋯O/Cl /H), see Fig. 4, similar to other weak interactions such as H-bonds [48, 49].

Conclusions

A systematic investigation of electronic structures and intermolecular interactions of sulfur in SHX(X = F, CN, Cl, Br, NO_2, CCH, CH_3, H) with HOCl have been presented. Up to three minimum configurations were found: a chalcogen-bonded complex, a hydrogen-bonded complex, and a halogen-bonded complex. Different approaches were employed to study the nature and strength of the resulting chalcogen bonds, halogen bonds and hydrogen bonds, which can be based on geometrical or AIM topological parameters, NBO analysis and vibrational frequency shifts, and localized molecular orbital energy decomposition analysis. The most electronegative substituent F cannot form hydrogen-bonded complexes, while the most electropositive substituent CCH, CH_3 and H cannot form chalcogen-bonded complexes. The chalcogen-bonded complexes for electron-withdrawing substituents F, CN, NC and NO_2 are more stable than halogen-bonded and hydrogen-bonded complexes, while the hydrogen-bonded complexes for less electronegative or electropositive substituents CCH, Br, CH_3 and H are more stable than chalcogen-bonded and halogen-bonded complexes. The vibrational analysis of the studied complexes shows a significant frequency red shift for the S–X bond in the chalcogen bond (except for X = NO_2 which is blue-shifting), for the O–H bond in the hydrogen bond and the O–Cl bond in the halogen bond.

References

1. Scheiner S (1997) Hydrogen bonding. Oxford University Press, New York
2. Jeffrey GA, Saenger W (1991) Hydrogen bonding in biological structures. Springer, Berlin
3. Desiraju GR, Steiner T (1999) The weak hydrogen bond in structural chemistry and biology. Oxford University Press, New York
4. Grabowski SJ (2006) Hydrogen bonding—new insights. Springer, Dordrecht
5. Thakur TS, Kirchner MT, Bläser D, Boese R, Desiraju GR (2011) Phys Chem Chem Phys 13:14076–14091
6. Peris E, Lee JCJ, Rambo J, Eisenstein O, Crabtree RH (1995) J Am Chem Soc 117:3485
7. Lipkowski P, Grabowski SJ, Leszczynski J (2006) J Phys Chem A 110:10296
8. Pauling L (1960) The nature of the chemical bond, 3rd edn. Ithaca, Cornell University Press
9. Grabowski SJ, Sokalski WA, Leszczynski J (2006) J Chem Phys Lett 422:334
10. Zordan F, Brammer L, Sherwood P (2005) J Am Chem Soc 127:5979
11. Politzer P, Murray JS, Concha MC (2007) J Mol Model 13:643–650
12. Politzer P, Lane P, Concha MC, Ma YG, Murray JS (2007) J Mol Model 13:305
13. Clark T, Hennemann M, Murray JS, Politzer P (2007) J Mol Model 13:291
14. Politzer P, Murray JS (2011) Cryst Eng Comm 13:6593–6596
15. Metrangolo P, Murray JS, Pilati T, Politzer P et al (2011) Cryst Growth Des 11:4238–4246
16. Bernard-Houplain MC, Sandorfy C (1973) Can J Chem 51:3640–3647
17. Metrangolo P, Neukirch H, Pilati T, Resnati G (2005) Acc Chem Res 38:386
18. Riley KE, Hobza P (2008) J Chem Theory Comput 4:232
19. Brinck T, Murray JS, Politzer P (1992) Int J Quantum Chem 44:57
20. Murray JS, Lane P, Clark T, Politzer P (2007) J Mol Model 13:1033–1038
21. Murray JS, Lane P, Politzer P (2007) Int J Quantum Chem 107:2286–2292
22. Murray J, Lane P, Politzer P (2009) J Mol Model 15:723
23. Mohajeri A, Pakirai AH, Bagheri N (2009) Chem Phys Lett 467:393–397
24. Scheiner S (2011) J Phys Chem A 115:11202
25. Politzer P, Riley KE, Bulat FA, Murray JS (2012) Comput Theor Chem 998:2–9
26. Scheiner S (2013) Acc Chem Res 46:280–288
27. Politzer P, Murray J, Clark T (2013) Phys Chem Chem Phys 15:11178–11189
28. Politzer P, Murray JS, Lane P, Clark T (2014) Top Curr Chem. doi:10.1007/128_2014_568
29. Rosenfield RE, Parthasarathy JR, Dunitz JD (1977) J Am Chem Soc 99:4860–4862
30. Guru Row TN, Parthasarathy R (1981) J Am Chem Soc 103:477–479
31. Alikhani E, Fuster F, Madebene B, Grabowski SJ (2014) Phys Chem Chem Phys 16:2430–2442

32. Alabugin IV, Manoharan M, Peabody S, Weinhold F (2003) J Am Chem Soc 125:59–73
33. Weinhold F, Landis C (2005) Valency and bonding: a natural bond orbital donor acceptor perspective. Cambridge University Press, Cambridge
34. Li AY (2007) J Chem Phys 126:154102
35. Frisch MJ, Trucks GW, Schlegel HB, Scuseria GE, Robb MA et al (2009) Gaussian 09. Gaussian Inc, Wallingford
36. Boys SF, Bernardi F (1970) Mol Phys 19:553–566
37. Bader RFW (1991) Chem Rev 91:893–928
38. Bader RFW (1990) Atoms in molecules, a quantum theory. Oxford University Press, Oxford
39. Popelier PLA (2000) Atoms in molecules. An introduction. Prentice Hall, Harlow
40. Matta CF, Boyd RJ (2007) The quantum theory of atoms in molecules: from solid state to DNA and drug design. Wiley-VCH, Einham
41. Keith TA (2011) AIMAll, version 11.08.23. TK Gristmill Software, Overland Park
42. Reed AE, Curtiss LA, Weinhold F (1988) Chem Rev 88:899–926
43. Glendening ED, Badenhoop JK, Reed AE, Carpenter JE, Bohmann JA, Morales CM, Weinhold F (2004) NBO 5.G. University of Wisconsin, Madison
44. Su P, Li H (2009) J Chem Phys 131:014102
45. Schmidt M, Baldridge W, Boatz KK, Elbert JA, Gordon ST, Jensen MS, Koseki JH, Matsunaga S, Nguyen N, Sus KA et al (1993) J Comput Chem 14:1347–1363
46. Szawomir J, Grabowski J (2011) J Phys Chem A 115:12340–12347
47. Bent HA (1961) Chem Rev 61:275
48. Sanchez-Sanz G, Trujillo C, Alkorta I, Elguero J (2012) Chem Phys Chem 13:496–503
49. Weinhold F, Landis C (2005) Valency and bonding. Cambridge University Press, Cambridge